JGR Biogeosciences

METHOD
10.1029/2024JG008591

Special Collection:
Quantifying Nature-based Climate Solutions

Novel Field Experiment on Alkalinity Enhancement in Intertidal Environments—A Trailblazer for Natural Climate Solutions

I. Mendes[1], J. Lübbers[1], J. Schönfeld[2], A. Baldermann[3], A. R. Carrasco[1], A. Cravo[1], A. Gomes[1,4], P. Grasse[2,5], and F. M. Stamm[3]

[1]Centro de Investigação Marinha e Ambiental (CIMA), Rede de Infraestrutura em Recursos Aquáticos (ARNET), Universidade do Algarve, Faro, Portugal, [2]GEOMAR Helmholtz-Zentrum für Ozeanforschung Kiel, Kiel, Germany, [3]Institute of Applied Geosciences, Graz University of Technology & NAWI Graz Geocenter, Graz, Austria, [4]ICArEHB—Interdisciplinary Center for Archaeology and Evolution of Human Behaviour, Universidade do Algarve, Faro, Portugal, [5]German Centre for Integrative Biodiversity Research Halle-Jena-Leipzig (iDiv), Leipzig, Germany

Abstract One recently proposed approach to reduce atmospheric CO_2 concentrations is marine alkalinity enhancement. This technique increases the CO_2 uptake capacity of seawater through weathering of fine-grained (mafic) rocks and minerals in marine environments. The weathering process has been extensively tested in laboratory studies and verified by numerical models. Field experiments scaling the CO_2 uptake under natural conditions are still lacking. In a methodological approach, a novel in situ experiment was designed and installed in a salt marsh at Ria Formosa coastal lagoon, southern Portugal. The experiment comprised deployments of different sizes of olivine and basalt substrates, and a control site, which were tidally submerged twice a day. A monthly monitoring scheme of supernatant and porewater properties from each deployment and control site was established, and procedures for temperature, salinity, oxygen, pH, total alkalinity, nutrient, and trace metal analyses were defined. This paper is devoted to the methods and describes the design, a protocol for the analyses, and an evaluation of experimental performance and reliability. Data from the first 6 months are presented for validation of the experiment. They demonstrated elevated total alkalinity in water samples, mostly in porewater after the deployments, while salinity, oxygen, and pH reflect the control conditions. Significant alkalinity differences were observed between the treatments and the natural background conditions monitored at the control site, during the 6 months of the experiment. The methodological approach is presented with strengths, limitations, and recommendations for an upscaling as CO_2 removal measure, servicing, and subsequent investigations.

Plain Language Summary Reducing atmospheric carbon dioxide (CO_2) concentrations to combat global warming is a major world challenge. A recently proposed approach to reduce atmospheric CO_2 is to increase ocean alkalinity. This technique increases the CO_2 uptake capacity of seawater by dissolving natural, fine-grained minerals in the marine environment. The dissolution process has been tested in the laboratory and verified by mathematical models, but field experiments under natural conditions are still lacking. To fill this gap, an in situ experiment was designed and installed in a salt marsh area, in the coastal lagoon of Ria Formosa, southern Portugal. Natural olivine and basalt substrates of different grain sizes were deployed, with an untreated control site for comparison. Monthly monitoring of water properties included measurements of temperature, salinity, oxygen, pH, total alkalinity, nutrients, and trace metals. Data of the first 6 months showed higher total alkalinity in the water samples, mostly in porewater, after the deployments, while the other environmental parameters remained stable. Significant alkalinity differences were observed between the treatments and the natural background conditions at the control site. The methodological study provides insights into the experimental design, analytical protocols, and performance evaluation, offering recommendations for scaling up, maintenance, and future studies for climate solutions.

Key Points:

- Implementation of a nature-based experiment for assessment of alkalinity enhancement as a climate solution
- Enhanced weathering of mafic rocks and minerals in salt marshes
- Description of the experimental design, implementation, sampling strategy, and analytical procedures of the in situ experiment

Supporting Information:

Supporting Information may be found in the online version of this article.

Correspondence to:

I. Mendes,
imendes@ualg.pt

Citation:

Mendes, I., Lübbers, J., Schönfeld, J., Baldermann, A., Carrasco, A. R., Cravo, A., et al. (2025). Novel field experiment on alkalinity enhancement in intertidal environments—a trailblazer for natural climate solutions. *Journal of Geophysical Research: Biogeosciences*, *130*, e2024JG008591. https://doi.org/10.1029/2024JG008591

Received 6 NOV 2024
Accepted 4 FEB 2025

Author Contributions:

Conceptualization: I. Mendes, J. Lübbers, J. Schönfeld
Formal analysis: I. Mendes, J. Lübbers, J. Schönfeld, A. Baldermann, A. R. Carrasco, A. Cravo, A. Gomes, F. M. Stamm
Funding acquisition: I. Mendes
Investigation: I. Mendes, J. Lübbers, J. Schönfeld, A. Baldermann, A. R. Carrasco, A. Cravo, A. Gomes, P. Grasse, F. M. Stamm
Methodology: I. Mendes, J. Lübbers, J. Schönfeld, A. Cravo

1. Introduction

One of the greatest challenges of humanity is to limit global warming to 1.5°C above preindustrial levels (UNFCC, 2015). Despite all efforts made during the last decades to reduce CO_2 emissions, the implemented political and technical measures are still insufficient to stop global temperature rise (IPCC, 2018; Rogelj et al., 2016). Carbon dioxide removal measures have emerged as a potential sustainable solution: atmospheric

Project administration: I. Mendes
Supervision: I. Mendes
Visualization: I. Mendes, J. Lübbers
Writing – original draft: I. Mendes, J. Lübbers, J. Schönfeld
Writing – review & editing: I. Mendes, J. Lübbers, J. Schönfeld, A. Baldermann, A. R. Carrasco, A. Cravo, A. Gomes, P. Grasse, F. M. Stamm

CO_2 is stored on land, in the ocean, or in geological reservoirs (e.g., Meier et al., 2022; National Research Council, 2015). These techniques still underly many uncertainties including CO_2 sequestration capacities, costs, benefits, and potential environmental risks (Fakhraee et al., 2023; Morrow et al., 2020). Enhanced weathering on continents and ocean alkalinity enhancement are measures with high potential to increase carbon uptake and storage, and likewise reduce ocean acidification (Bach et al., 2019; Bellamy et al., 2012; Kowalczyk et al., 2024). In particular, silicate mineral weathering increases the natural alkalinity of seawater by releasing cations and binding CO_2 as bicarbonate and carbonate ions, thus increasing the gas exchange of CO_2 from the atmosphere to the ocean (Feng et al., 2017; Meysman & Montserrat, 2017). This process could be enhanced by spreading crushed reactive mafic rocks and minerals (e.g., basalt and olivine), in the marine environment (e.g., Bach et al., 2019; Köhler et al., 2013; Montserrat et al., 2017). The consumption of atmospheric CO_2 during mineral dissolution will depend not only on the reactivity of the silicate minerals of the materials used, but also on factors such as grain size, temperature, and pH (Hangx & Spiers, 2009; Hartmann et al., 2013). Despite promising results obtained by laboratory and modeling studies (e.g., Bach et al., 2019; Fuhr et al., 2022; Montserrat et al., 2017), little is known about the CO_2 uptake efficiency, nutrient release rate, and ecological effects of increasing the alkalinity in marginal marine environments. In particular, field experiments under natural conditions are still missing.

Based on model calculations, deployments of coarse-grained olivine in high-energy environments have been proposed (Meysman & Montserrat, 2017). The permanent redeposition in the surf zone abrades the grains and thereby removes reaction products from the grain surfaces, which sustains the solubility of the grains (Schuiling & Boer, 2011; Walker, 1992). For the open ocean, the deployment of 1-µm sized olivine is proposed on main shipping routes through the release in suspension with the ballast water of the vessels (Köhler et al., 2013). The smaller size ensures that the grains are readily dissolved in the surface mixed layer of the ocean before they sink to greater depths. The main disadvantage of both approaches proposed is that the materials are "out of contro" once they have been deployed. For example, parts of the grains may be deposited before dissolution, as beach sands at highly dynamic coasts, or get removed out of the surf zone by rip currents (e.g., Balouin et al., 2005; Poate et al., 2014; Wright & Short, 1984). Mineral dust particles may be covered with biofilms and subsequently get enclosed in marine snow aggregates, which rapidly sink from the photic zone, creating an own, immediate chemical and microbial environment (e.g., Simon et al., 2002; van der Jagt et al., 2018). Surveillance and monitoring of the reaction paths as well as sampling or recovery of the deployed material is therefore not possible.

Deployments in coastal areas can be serviced, monitored, and eventually remediated. However, they are prone to sediment instability, erosion, or accumulation, subjected to variable hydrodynamics, and sometimes human interference. For this reason, only areas of high environmental stability need to be considered as deployment fields. The pioneer vegetation zone of salt marshes adjacent to mud flats in sheltered bays or coastal lagoons is one of the most suitable areas. In the Ria Formosa coastal lagoon, southern Portugal, the pioneer zone has been identified as an area of high environmental stability (Schönfeld & Mendes, 2022). Long-term monitoring, including leveling, infers that a net sediment accumulation does not take place (Carrasco et al., 2021). The homogenous thicket of *Spartina maritima* (also referred to as *Sporobolus maritimus*) plants effectively reduce the hydraulic energy during flood and ebb tides (e.g., Allen, 2000), which inhibits reworking and erosion of artificial substrates after deployment.

This methodological study describes the design, monitoring scheme, and performance of a novel field experiment installed in a natural intertidal environment, consisting of three separate replicates. Nonharmful natural materials, such as reactive volcanic rocks rich in olivine, pyroxene, and plagioclase, commercially designed as olivine and basalt, were deployed in pine wood frames, previously installed in the pioneer vegetation zone at Ria Formosa coastal lagoon. The mineral olivine has the highest potential to sequester CO_2 (approx. 1 *t* CO_2 per 1 *t* olivine, Renforth & Henderson, 2017) but can impact the environment with heavy metals (e.g., Ni; Guo et al., 2022). The CO_2 sequestering capability of the mafic volcanic rock basalt is approximately 30% less than pure olivine or peridotite, but basalt can be enriched in nutrients and essential elements (e.g., P, Ca, K, Si, and Zn; Strefler et al., 2018), potentially acting as slow-releasing fertilizer. The overarching scientific questions of this field experiment were (a) whether the lithic substrates produce excess alkalinity under natural conditions; (b) to what extent the alkalinity is delivered to the (pore)waters within the salt marsh pioneer vegetation zone; and (c) how long the weathering process of the deployed substrates is active.

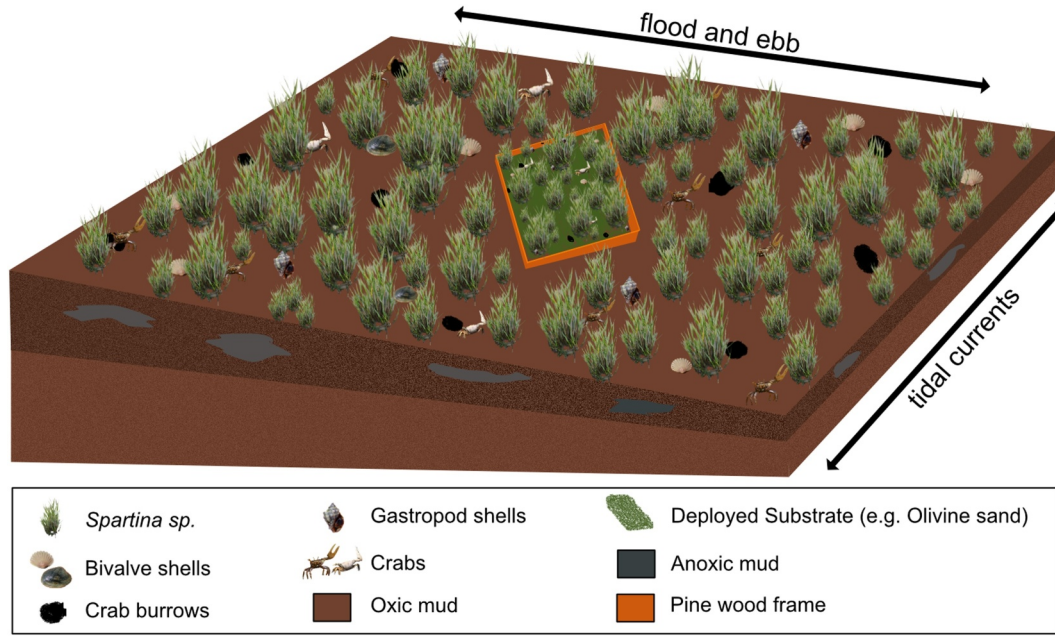

Figure 1. Schematic sketch of the experiment field installation in the salt marsh pioneer zone (not at scale).

2. Materials and Procedures

2.1. Experimental Design and Implementation

The concept of the experimental approach is to bind the individual treatments with wooden frames, which act as low barriers and prevent substrate dispersal by tidal currents or wave action. They also create controlled conditions for measurements and observations. The frames with 60 × 60 cm width, were made from planed pine wood boards, with 18-mm thickness and 135-mm height. They were assembled before installation. A simple, angular woodworking joint was applied. Angular joints respond ductile in two directions, which is important once reactive forces occur during installation. Three SPAX® INOX screws, 4 × 40 mm, countersunk head, *T*-star Plus T20 drive, and stainless steel A2, 1.4567, were used as fastener on each corner. For further stabilization, the four inner corners of the box were reinforced with a triangular wooden ledge, which was fastened with four SPAX® INOX screws, 3 × 30 mm, countersunk head, *T*-star Plus T10 drive, and stainless steel A2, 1.4567. The A2 alloy has been proven to be noncorrosive in seawater, both under oxic and anoxic conditions in the intertidal zone. Furthermore, the screws are self-drilling due to the 4 Cut tip and do not splinter pine wood. The frame structure was not treated with preservatives or paint.

Before installation, the frames were laid out on a representative place in the *Spartina* field. The place was chosen by integrating all features that do occur in the vicinity, where the vegetation coverage was considered as being largely homogenous, and where the ubiquitous surface undulations were lower. Physical surface disturbances, such as crab holes or gutters, were avoided. The frames were oriented with their diagonal axes perpendicular to the slope (Figure 1), as tidal currents split at the corners otherwise and would not be substantially decelerated by the frames.

Turbulence can therefore be considered as minor and would only affect the area around the corners outside the frames. Before installation, a notch was cut with a spade around the frames to cut the roots of the vegetation. The frames were driven into the notch by using a rubber mallet until they stuck out approximately 2–3 cm, maintaining a penetration depth of about 10 cm in the sediment. They were aligned horizontally as much as possible by using a bubble level. In most places, the sediment surface was slightly tilted toward the mud flat and the tidal channel. Consequently, the upper landward corner of the frame was about 1–2 cm above the ambient sediment surface, and the lower seaward corner stuck out about 2–4 cm. Each frame was tagged with a planting sign in the top right corner (seaside) and labeled with information about the project and the treatments applied.

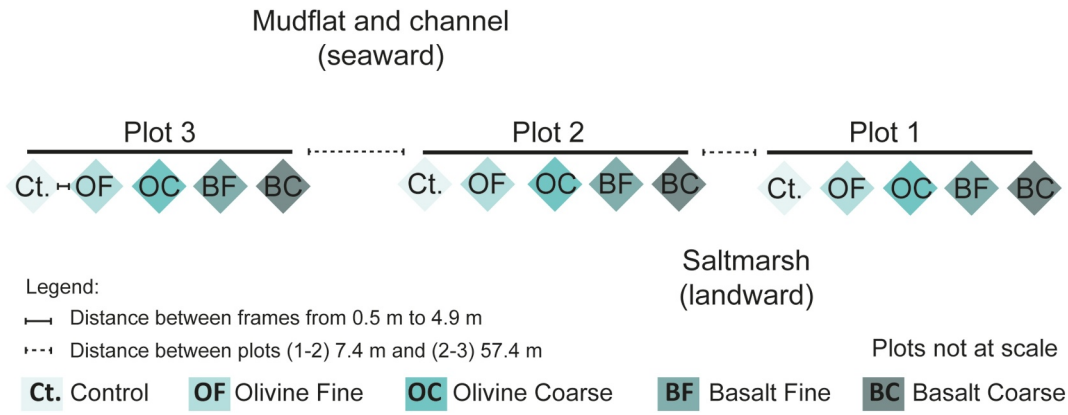

Figure 2. Schematic representation of the field experiment, composed by three plots, each one with the five experimental treatments installed in the salt marsh pioneer zone.

Three replicate sites (plots) were installed, each one containing five separated experimental fields. One field was covered with fine-sized basanite designated as basalt fine (BF), one with coarse-sized basanite as basalt coarse (BC), one with fine-sized picrobasalt rich in olivine as olivine fine (OF), and another with medium-sized picrobasalt rich in olivine as olivine coarse (OC). A fifth field was left untreated as control (Ct.) (Figure 2).

2.2. Procedures Before Implementation

2.2.1. Grain Size and Mineralogical Composition of the Deployed Minerals

Sand-sized materials were given preference for the treatments because of their high permeability and easier handling when spread across the experimental fields. Reactive mafic volcanic rock powders (olivine-rich picrobasalt and basanite) commercially available as olivine and basalt, were used. These materials are produced by milling and sieving in quarry works. Norwegian olivine (i.e., picrobasalt) was supplied by SCR-Sibelco NV, Antwep, Belgium. As for this study, grade AFS 120 (90–180 μm) and grade AFS 50 (180–355 μm) were selected, representing fine and medium to coarse sand fractions, respectively. Basalt (i.e., basanite) was purchased from Rheinische Provinzial-Basalt-und Lavawerke GmbH & Co. oHG, Sinzig, Germany. The technical quality "Durubas" (0.02–2.2 mm) and the fine fraction (63–355 μm) obtained by dry sieving with a 355-μm mesh were used. This fraction comprised only ∼28% of the bulk "Durubas" products. The quality "Basalt Fugensand" (0.5–1.0 mm) met our requirements and was used without further treatment (Figure 3).

The mineralogical and the major elemental composition of the raw materials were also obtained (Table 1). The mineralogical composition was determined via Rietveld refinement of X-ray diffraction patterns recorded on a PANalytical X'Pert PRO diffractometer (operational conditions: Co-Kα, 40 kV, and 40 mA) equipped with a high-speed Scientific X'Celerator detector. The PANalytical X'Pert HighScore Plus software package and a PDF-4 database were used for mineral identification and quantification. The analytical error is <2 wt.% for each mineral phase, based on comparison with chemical data (Baldermann et al., 2021). The samples OC and OF have a high olivine content (>92 wt.%), with minor pyroxene, amphibole, and clay minerals, whereas samples BC and BF are characterized by higher amounts of pyroxene and plagioclase (total: ∼68–73 wt.%) and moderate contents of olivine, orthoclase, and smectite (total: ∼24–29 wt.%).

The major elemental composition of the raw materials, prepared as standard powder pellets, was analyzed by energy-dispersive X-ray fluorescence using a PANalytical Epsilon 4 X-ray spectrometer (Table 1). The analytical error is ±0.5 wt.% for the major elements, as determined by replicate measurements of a range of USGS standards (Abdullayev et al., 2021). The chemical composition of these materials in the total alkali versus silica diagram, which is frequently used for the classification of volcanic rocks (Le Maitre, 2005), identifies OC and OF as picrobasalt and BC and BF as basanite, respectively, which is consistent with the nomenclature we used for the characterization of the raw materials.

Before deployment, the materials were again checked for purity and dryness, and the dry bulk density was obtained, with 1.58 for OF, 1.67 for OC, 1.51 for BF, and 1.29 g cm^{-3} for BC.

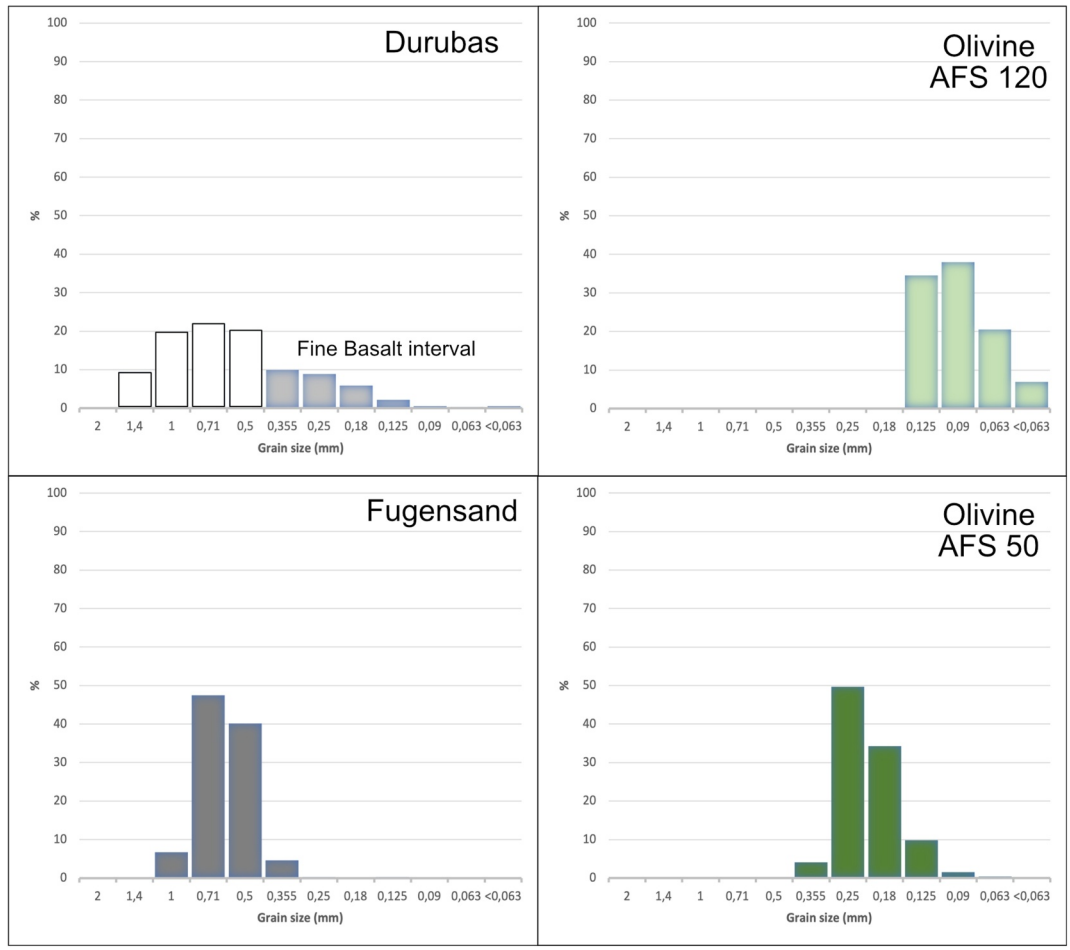

Figure 3. Grain size distribution of the starting materials used in the experiment, Durubas, Fugensand, Olivine AFS 120 and Olivine AFS 50.

2.2.2. Bottle Experiments to Test Nickel Release and Material Deployment

To assess the potential nickel (Ni) release during dissolution and to secure minimum environmental quality standards (EQS) for seawater, raw material was tested in the laboratory before deployment. Five acid-cleaned glass bottles (1 L) were filled with 0.8 L of filtered seawater from the study site, the different substrates to be tested were added, and a fifth bottle was left as a control (for details, see Text S1 in Supporting Information S1). The bottles were permanently shaken and sampled over 10 days. The elemental analyses were carried out using an Agilent 7900 inductively coupled plasma mass spectrometry by using standard methods for trace metals analyses of near-coastal waters. The accuracy of the certified reference material (BCR505; EU, JRC) was 10%, and the precision was lower than 5%.

The EQS value for Ni in marine waters according to the European Commission report is 34 $\mu g L^{-1}$ (Table S1 in Supporting Information S1). This value was only exceeded shortly in the beginning of the experiment in the fine fraction of olivine and basalt (Figure S1 in Supporting Information S1). The higher concentrations of Ni in the fine substrates at the beginning of the laboratory experiment were probably related to very small, fast dissolving minerals (e.g., smectites) present in the raw material. The raw material used in both, bottle experiment and deployment, was not previously washed to simulate real deployment scenarios. Considering that the laboratory experiment was done in a close bottle and the in situ experiment was conducted in an intertidal area, tidally submerged twice a day with water renewal, a potential risk of environmental contamination seems unlikely.

Encouraged by the results of the above leaching experiment, the basalt sand was applied as a layer of 1 cm and the olivine as a layer of 0.5 cm thickness. The amount of material was calculated from the geometric volume of the

Table 1
Mineralogical and Chemical Composition of the Raw Materials Used in the Experiment: Basanite is Denominated as Basalt and Olivine-Rich Picrobasalt as Olivine

Mineralogical composition				
	Comp. (wt.%)			
Phase	Basalt coarse	Basalt fine	Olivine coarse	Olivine fine
Amphibole	-	-	0.7	0.8
Chlorite	-	-	1.2	0.5
Talc	-	-	0.4	0.4
Olivine	10.1	13.5	93.0	92.3
Pyroxene	42.5	40.3	4.4	5.6
Biotite	0.7	0.8	0.3	0.4
Smectite	6.3	6.0	-	-
Analcime	2.7	2.3	-	-
Plagioclase	28.6	28.1	-	-
Orthoclase	9.1	9.0	-	-
Chemical composition				
	Conc. (wt.%)			
Component	Basalt coarse	Basalt fine	Olivine coarse	Olivine fine
SiO_2	43.7	43.2	41.4	42.8
Al_2O_3	14.2	13.3	0.8	0.4
CaO	9.7	9.3	<0.1	0.1
MgO	10.3	12.5	48.0	48.2
Fe_2O_3	11.7	12.0	8.8	7.3
K_2O	1.4	1.4	<0.1	<0.1
P_2O_5	0.7	0.7	<0.1	<0.1

frames and the dry bulk density. In particular, 5.5 of BF, 4.6 of BC, 2.8 of OF, and 3 kg of OC were preweighed for each experimental field and individually packed in bags before deployment. The spreading was done by two people crouching around the wood frame. They took the respective raw materials out of the bag with small, plastic toy shovels, and sprinkled it over the entire field. Lateral inhomogeneities by individual preferences on how to sprinkle were thereby equalized. The layer thickness may nonetheless vary slightly in places, in particular, where the falling materials was deflected by the leaves of the *Spartina* grass. Grains that have fallen on the frame were brushed inside. Only a negligible amount fell outside the frame and was lost.

2.3. Sampling and Analytical Procedures

An analytical and sampling scheme was designed to obtain the environmental data sets necessary to answer the scientific questions of the field experiment. While the alkalinity is the focus of the experiment, the determination of carbonate system parameters, such as $\Omega_{calcite}$ or ρCO_2, are likewise of interest. Therefore, critical environmental parameters, as temperature, salinity, dissolved oxygen, and specific nutrients were measured to facilitate the calculation of carbonate system parameters (Lewis & Wallace, 1998).

Silicate minerals are considered to weather very slowly under ambient temperature conditions (Hangx & Spiers, 2009; Montserrat et al., 2017; Vink & Knops, 2023), but they have been proven to be quite reactive in seawater (Flipkens et al., 2021; Fuhr et al., 2022; Meysman & Montserrat, 2017). Therefore, the first water samples were taken one day after material deployment, and monthly from there on. The sampling was always performed around the middle of a month, depending on tidal range conditions, daylight and the weather conditions (e.g., avoiding rain conditions or too high temperatures). The samples were collected during the ebb period of the first low tide after sunrise, because the oxygenation, pH, and carbonate system parameters in near-surface porewaters show a high diurnal variability in salt marshes (Baumann et al., 2015; Koop-Jakobsen et al., 2018; Saderne et al., 2013; Schunter et al., 2020). The porewater sampling was performed shortly after the sampling sites have emerged to avoid bias by desiccation (Schönfeld & Mendes, 2022). During each water sampling campaign, a site description was made for each experimental field, including photographs, assessment of vegetation cover (in percent), *Spartina* height (minimum, maximum, and average), description and count of visible macrofauna (live and dead), sediment disturbance due to faunal activity (e.g., crab or worm holes), and other visible features. The number of *Spartina* shoots in each experimental field was also counted regularly. In addition, data on air temperature, rainfall, and wind conditions were recorded by a meteorological station at Faro Airport. The data were made available by the Portuguese Institute of Sea and Atmosphere (https://www.ipma.pt/pt/oclima/monitoriza.dia/). A serious matter of sampling and experiment surveillance are the vast number of footprints that were left in the muddy salt marsh sediments, which comprise mainly of clay minerals (mostly muscovite and minor kaolinite), feldspar, quartz, pyrite, and an amorphous phase, interpreted as organic matter and diatom-associated bio-opal content. The footprints can be up to 30 cm deep, exposing the anoxic zone of the sediments, thereby releasing nutrients, alkalinity, and potentially trace metals. The trampling also creates excess suspension that is redistributed locally during the next flood. To avoid these disturbances, and to go easy on the salt marsh vegetation, the experimental sites were accessed by walking on sporting body boards.

Supernatant water and porewater were sampled in each experimental field, and lagoon water was collected in front of each plot. Water samples were taken with precleaned and acid-decontaminated (HCl, 10%) vials or syringes, depending on water availability, and stored in precleaned and acid-decontaminated vials of two types: 20 ml, high-density polypropylene Zinsser vials (Ø × *A*: 27 × 60 mm, VWR, No. 218–2255) and 100 ml polypropylene beakers (Ø ext.: 52 mm, VWR, No. 216–1824). Lagoon water samples used for on-site measurements were taken with precleaned 100 ml polypropylene beakers (Ø ext.: 52 mm, VWR, No. 216–1824).

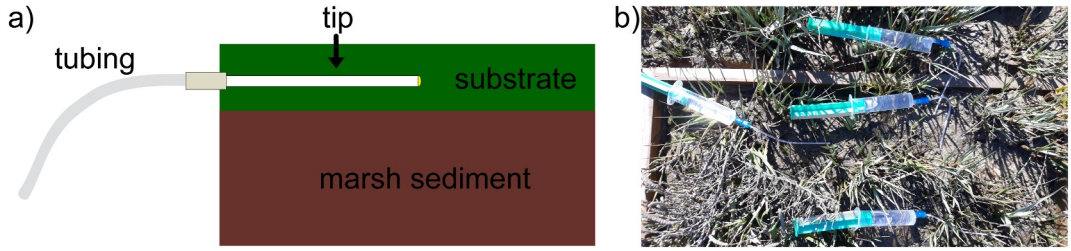

Figure 4. (a) Schematic representation of the porewater sampling strategy used and (b) a field image of four rhizons on an experimental field.

Supernatant water samples were regularly taken from a puddle that is kept in the lower corner of the wooden frame of the experimental field, during falling tide. Hundred ml of water was collected for trace metal and nutrient analyses, another 100 ml was taken for on-site measurements, and 20 ml for alkalinity analysis. The vial of the latter sample was carefully filled to avoid air bubbles and degassing of CO_2. On-site measurements were immediately performed using a WTW Multi 3620 IDS multiparameter probe, and the remaining samples were stored in a cooler with ice packs and promptly transported to the laboratory for further analyses.

Porewater samples were collected with rhizon samplers (Schönfeld & Mendes, 2022; Seeberg-Elverfeldt et al., 2005). The rhizon extraction method was chosen instead of centrifugation or high-pressure squeezing, as dissolved oxygen concentrations are not altered in this way (Anschutz & Charbonnier, 2020; Schulz, 2006), and the sediment is not to be taken out of the experimental field. Four rhizons randomly orientated were used per experimental site. During warmer months, 5 rhizons were used to shortly collect larger volumes and to minimize effects arising from evaporation. Rhizons were horizontally inserted in the upper 0.5–1 cm layer of the sediment, close to small depressions, or small bumps of the sediment surface, in which the tip is placed and kept stable in the surface of the applied substrates (Figure 4). In the control experimental fields, the rhizon tips were placed in the oxic surface layer of the sediment. An acid-cleaned, 20 ml syringe was plugged to the luer-lock connector of the tubing; the syringe piston was pulled to generate a vacuum and held open with a spacer slat (Seeberg-Elverfeldt et al., 2005). The pore size of the rhizons was 0.1 µm. About 15 ml porewater was collected in ~60 min on average per rhizon. The porewater was distributed in four 20 ml vials for on-site salinity, oxygen, and pH measurements, as well as for subsequent alkalinity (sampled without bubbles) and trace metal and nutrient analysis. Further, the in situ temperature was measured at the extraction site using a plug-in thermometer inside the surface sediment layer. The samples for alkalinity, nutrients and metal analyses were immediately stored and transported to the laboratory in a cooler filled with ice packs. Lagoon water samples were taken from the surface of the channel in front of each plot, during the falling tide (ebb), before supernatant sampling, and during the rising tide (flood) after porewater sampling.

The salinity, oxygen, and pH of the lagoon channel, supernatant, and porewater samples were measured on-site with a WTW Multi 3620 IDS multiparameter probe. The pH sensor was calibrated on every sampling day with pH 4, 7, and 10 buffer solutions (pH 4: YSI-381, pH 7: YSI-3822, and pH 10: YSI-3823). The buffer solutions have an accuracy of 0.002 units at 25°C according to the manufacturer's data instructions. They are compatible with National Institute of Standards and Technology pH standards. The accuracy of the conductometer sensor (IDS digital conductivity cells TetraCon® 925) was tested in advance of the measurements with an International Association for the Physical Sciences of the Ocean (IAPSO) standard (34,994 salinity units at 15°C). If necessary, the sensor was recalibrated with 0.01 mol/l KCl, 1.413 µS cm^{-1} at 25°C, following the procedures of the user manual. The calibration of the oxygen sensor was checked every time before sampling, which is self-calibrating according to the manual.

The alkalinity was measured on the same day of sampling by using the Bruevich's titration method, which is particularly designed for small sample volumes (Pavlova et al., 2008; Wallmann et al., 2006). The accuracy of the alkalinity method was verified by the "Test for linearity" over a period of 3 days, which yielded a linearity of $R^2 = 0.995$ (see Supporting Information S2). One ml of the sample, 2 ml distilled water, and 20 µl methyl red and methylene blue indicator solution were poured into a Pavlova titration vessel. The solution was titrated with 0.02 M HCl until a stable pinkish color was established. To avoid a stochastic bias related with the different perceptivity and recognition of the pink color tipping point, only one person measured all the samples of one campaign. The

Table 2
Two-Way Analysis of Variance of the Oxygen Saturation (%) in Porewater Over the First Six Months of the Experiment

Two-way ANOVA (oxygen)						
Source of variation	*Sum of squares (SS)*	Degrees of freedom (df)	Mean sum of squares (MS)	F-value	P-value	F crit
Between the treatments	2.2436	4	0.5609	0.9432	0.4478	2.5787
Between the plots	2.2758	2	1.1379	1.9136	0.1594	3.2043
Interaction between treatments and plots	0.5227	8	0.0653	0.1099	0.9987	2.1521

titration vessel was continuously flushed with nitrogen (N_2) to expel the reaction products CO_2 and H_2S from the sample solution. An IAPSO standard with a total alkalinity of 2.325 mmol/l was measured in triplicate before, and after a sample series. Each seawater sample was analyzed in triplicate as well. Mean values were calculated, the measured values from the samples were corrected with the target value of the IAPSO standard, and the total alkalinity was calculated with standard formulas (Wallmann, 2023). The internal alkalinity standard was stable for 2 months and was routinely replaced thereafter. The alkalinity of the IAPSO seawater and the Dickson alkalinity standard were routinely measured for calibration and yielded a standard deviation of 0.0036 µM.

The nutrient samples were filtered after collection through a 0.45-µm membrane filter (Whatman, ME 25/21 ST, 0.45 µm, Ø 47 mm) and frozen at −20°C for preservation. Ammonium (NH_4^+), nitrate (NO_3^-), phosphate (PO_4^{3-}), and silicic acid ($Si(OH)_4$) were analyzed by spectrophotometric methods as described in Grasshoff et al. (1999), using a Thermo Scientific™ Sectrophotometer, Model Evolution 201. The Marine Nutrient Standards Kit (OSIL) was used as a reference standard, which guarantees a high accuracy of concentration measurements. The detection limits for the analyzed nutrients were 0.09 µM for NH_4^+, 0.07 µM for NO_3^-, 0.03 µM for PO_4^{3-},and 0.05 µM for $Si(OH)_4$.

The water samples for trace metals (e.g., Ni, Cu, and Cr) were filtered through precleaned and acid-decontaminated (HCl, 10%) 0.45-µm membrane filters (Whatman, ME 25/21 ST, 0.45 µm, Ø 47 mm), and afterward acidified with ∼0.5 ml of nitric acid (67% HNO_3) for preservation.

3. Experimental Assessment

The concept and applicability of the methods used in the field experiment were assessed in the pioneer salt marsh vegetation zone at the Ria Formosa wetland, designed as a marine field experiment. Three independent replicate plots were installed at large distances, and each plot comprised five experimental fields bounded by pine wood frames (Figure 2). The sediment surface of the experimental fields was covered with reactive mafic rock powders, that is, fine and coarse basalt or olivine. The fifth field was left untreated as control. The experiment was performed to test (a) whether the substrates produce enhanced alkalinity under natural conditions, (b) to what extent the alkalinity contributes to the lagoon waters, and (c) how long the substrates are active.

A two-way analysis of variance (ANOVA) was carried out to examine the effect of different treatments compared to natural conditions and between replicates (plots). The results of the analysis showed no statistically significant differences ($p > 0.05$) between the replicates, over the first 6 months of the experiment (Table 2). Using the percentage of dissolved oxygen saturation in porewaters as an example, data did not vary between the treatments and the control boxes ($p = 0.4478$) in the three replicate plots, following a subsequent two-sample t test to find differences between each plot comparing the control samples with the different treatments. The results showed no significant differences between the control plots, with p-values of 0.45 for P1 control versus P2 control and 0.6 for P1 control versus P3 control. Consequently, the deployment of different substrates in the three plots did not have an effect on the dissolved oxygen saturation levels compared to the control conditions.

The two-way ANOVA, based on the mean and median alkalinity values calculated by averaging the measurements in porewater from all three plots, over the first 6 months, revealed statistically significant differences between the treatments and natural conditions, indicating that the treatments increased alkalinity compared to the background levels. This was further confirmed by a two-sample t test, which compared the control to each treatment, with p-values <0.05 (Table 3).

Table 3
Two-Way Analysis of Variance on Alkalinity Measurements in Porewater Over the First Six Months of the Experiment, Along With the Results of a Two-Sample t test Comparing the Control With the Treatments

Two-way ANOVA (alkalinity)							Two-sample *t* test	
Source of variation	*Sum of squares (SS)*	Degrees of freedom (df)	Mean sum of squares (MS)	F-value	P-value	F crit	*Control* versus.	P-value
Between the treatments	9.8607	4	2.4652	2.7208	0.0357	2.4937	Olivine coarse	0.0178
Between the plots	0.2877	2	0.1439	0.1588	0.8535	3.1186	Olivine fine	0.0340
Interaction between treatments and plots	3.7400	8	0.4675	0.5160	0.8409	2.0644	Basalt coarse	0.0036
							Basalt fine	0.0307

Plot 2 was chosen here as an arbitrary example, because no differences were found between plots. The data showed elevated total alkalinity for the first 6 months, more evident in porewater in all treatments except for the control, while the other environmental parameters, for example, salinity, oxygen, and pH remained relatively similar as compared to control conditions ($p > 0.05$), with recognition of seasonal variations (Figure 5). An exception was the lower salinity values in December 2022. They were associated with a precipitation event that occurred a few days before water sampling. The highest alkalinity values were observed after the first day of deployment, which is due to the high reactivity of the finest fraction of the substrates supplied in the different treatments. The fine particles are likely to weather faster, explaining the observed strong increase in alkalinity and pH of the porewater. After the fine particles are weathered, the coarser particles continue to weather, though at a slower rate, and therefore steadily increase the alkalinity and pH of the water. The untreated control depicted no elevated alkalinity ($p > 0.05$) but showed a slight decrease from September to December 2022, covarying with temperature, and probably reflect some of the seasonal dynamics in natural alkalinity production (e.g., Reithmaier et al., 2023). The outlier of high pH and low alkalinity values in the control box in January 2023 can either be attributed to a transient coverage with mats of *Enteromorpha* algal filaments, which may change the pH due to photosynthesis/night respiration, or to an accidental influence of unseen crab and/or other animals excretion

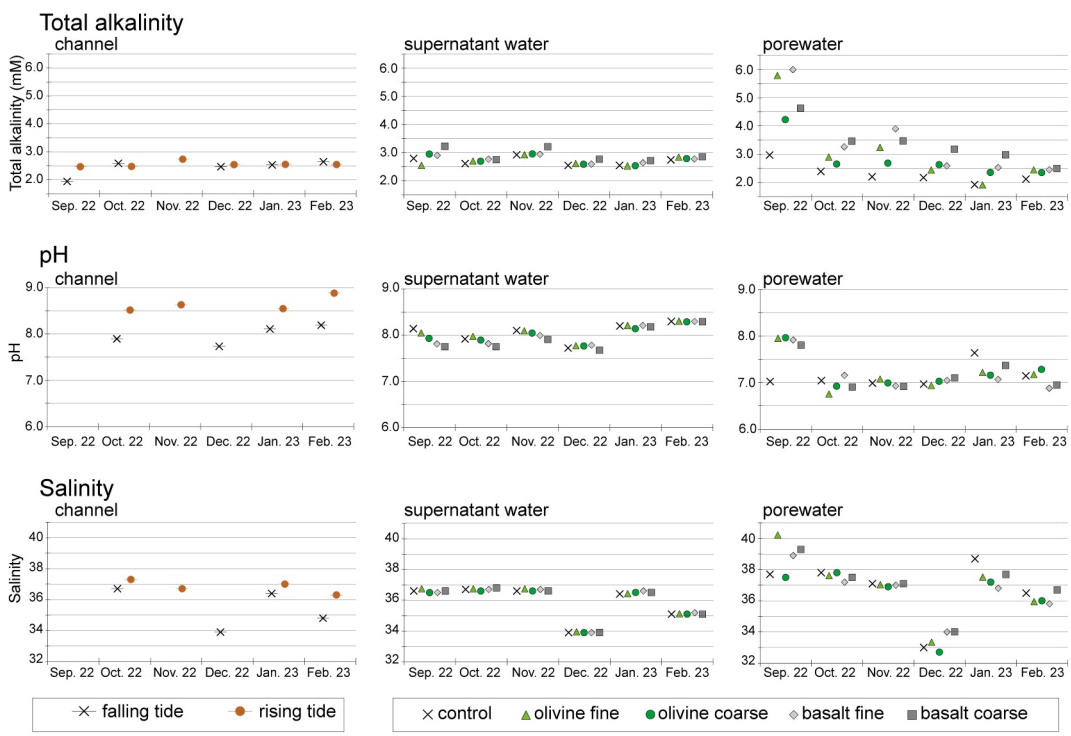

Figure 5. Records of total alkalinity, pH, and salinity measured in the supernatant and porewater samples from plot 2 and from the channel during falling and rising tide, for the first 6 months of the experiment.

products at the porewater sampling spot. Moreover, it is important to remark that the water collected for alkalinity analysis is not the same as for in situ pH measurement. The different treatments and grain sizes used showed consistent results among the three replicate plots, with no differences between them ($p > 0.05$). The efficiency of the treatment with different substrates was displayed by the pervasive alkalinity gradient between the supernatant water and the porewater. As the alkalinity was always higher than in the control box, the gradient depicts steady alkalinity production by the substrates and a slow diffusion to the supernatant waters in puddles at the lower corner of the boxes. The exposure time of a few hours of tidal emersion was sufficient to affect higher alkalinities than in the adjacent tidal channel. In combination with the alkalinity of the tidal channel water, the gradient even offers constraints of alkalinity variability, even though they may change through time with upcoming and outgoing waters and seasonality (Figure 5).

From these alkalinity data, mineral-specific dissolution rates can be calculated, as is exemplarily shown for the chemical weathering of the primary silicate mineral wollastonite (=pyroxene, $CaSiO_3$): $CaSiO_3 + 2CO_2 + 3H_2O \rightarrow Ca^{2+} + 2HCO_3^- + Si(OH)_4$.

It becomes evident that atmospheric CO_2 is consumed during this process and that carbonate alkalinity is generated, causing a reduction of 1 mol of atmospheric CO_2 per 1 mol of HCO_3 formed. Such calculations will allow us to verify and quantify (a) the efficiency of the individual substrates and (b) the carbon sequestration potential at the Ria Formosa marsh system.

4. Experiment Strengths and Limitations

Several strengths can be outlined from the employed procedures in our experiment that provides means to its replication in other intertidal environments. The substrates were, to our best knowledge, not eroded by tidal currents or small waves affecting the frames. No negative physical interference of the frames with the sedimentary environment was observed, nor erosion at their edges, which again demonstrates the pioneer vegetation zone with *Spartina* as a suitable place for the experiment. The employed method for supernatant and porewater sampling guarantees the collection of sufficient sample amounts for analysis. The applied grain size fraction of the substrates provided sufficient pore space and permeability to allow exchange with the water above. The irregular surface morphology around the plants was of advantage for porewater sampling. The consumables and instruments needed to perform the field experiment are cheap and easy to purchase. The installation in the salt marsh is easy, and it takes only 2 days to accomplish the setup. However, accessibility to the salt marsh, the logistics, and man power matters on sampling dates. This mainly concerns the tidal cycle, which offers only a limited period when field data collection is possible.

A limitation of the field experiment is related to the size of the experimental fields. Earlier studies proposed an upscaling of field trials to areas of 100 m^2 and the use of common dredging equipment (Montserrat et al., 2017). Our frames were 0.36 m^2, hence more than two orders of magnitude smaller. The substrates form a thin veneer, which can be accumulated in small depressions between the *Spartina* plants. The exact thickness of the substrate layer is therefore difficult to measure, and it is probably not constant through time. A faint coverage with mud was recognized after several months in some parts of the experimental fields, which are likely derived from bioturbation from crab holes and worms' excrement. Transient, patchy, and golden-brown diatom and cyanobacteria mats were observed after 1 month. A seasonal coverage during winter months of the whole pioneer zone of the salt marsh by filamentous *Enteromorpha* macroalgae also occurred and potentially hampered the weathering of the substrate. Some salt marsh vegetation can be damaged by even walking on bodyboards in the experimental sites, and surface sediment disturbances can occur, especially outside the field treatments, from where the samples are collected. The boards should be used for displacement in the experimental area from the first day. Another limitation of the process efficiency lies in the influence of natural conditions. While the concept of ocean alkalinity enhancement is designed to operate under natural circumstances, numerous environmental factors that could potentially interfere with the process's efficiency are unpredicted and often not considered. Examples of such factors include storm events, which may lead to increased sedimentation rates or erosion, and bioturbation, where organisms such as crabs or worms burrow into the substrate, hindering rapid weathering. Unforeseen processes like these are difficult to predict, but must be considered when implementing such experiments. Recent studies emphasize the importance of carefully considering deployment strategies and monitoring frameworks to mitigate potential environmental risks and optimize efficiency in natural ecosystems. For instance, storm-induced sedimentation could cover the substrate with a mud veneer and slow down weathering processes, while

bioturbation may redistribute or bury material, reducing its exposure to reactive conditions (e.g., Fakhraee et al., 2023). Transient or seasonal phenomena, such as algal blooms or diatom mats, could also form and interfere with substrate weathering. These factors emphasize the complexity of scaling up the process and highlight the importance of comprehensive experimental design and monitoring to mitigate their impacts. The results of our field experiment, performed in nature, under natural environmental conditions, disagree with laboratory experiments conducted in closed systems. The laboratory experiments showed a rapid increase of alkalinity in two to 6 days and rather constant values thereafter (Montserrat et al., 2017), or a moderate increase within 2 days and subsequently declining alkalinity to values far below the initial alkalinity (Fuhr et al., 2022).

5. Comments and Recommendations

The new experimental design offers not only the investigation of hydro-chemical properties but also an assessment of the influence of the treatments on carbonate system parameters. Furthermore, it allows the investigation of real-world faunal and floral responses to mineral/rock powder deployments in the coastal zone. This is a breakthrough advance in comparison with laboratory or closed system mesocosm experiments.

An important question that could not be solved to date is the leaching, bioavailability, accumulation, and fate of critical trace metals derived from substrate dissolution. The constrained experimental design and multiple options for sampling will allow to address this question, which is of particular importance for upscaling and application as novel carbon sequestration technology for climate solutions.

Another unsolved question concerns the positive effects on the salt marsh vegetation. Finely ground basalt is extensively used as fertilizer in agriculture. Studies with olivine-rich substrates have shown that it increases the soil water pH and the plant biomass (Ten Berge et al., 2012). A regular monitoring of the *Spartina* shoots and an assessment of their growth dynamics over a year will provide further constraints on the long-term effects on the vegetation coverage.

Finally, the remediation after the experiment is a yet unsolved issue. While the frames may be pulled out easily, the substrate cannot be retrieved without major damage to flora and fauna, neither with a scraper nor with a vacuum cleaner. Replanting and surface coverage with pristine mud may be necessary. These measures will create damage in another place or imply the availability of donor sites in the Ria Formosa wetland system. However, and according to our present knowledge based on observations and preliminary trace metal measurements, the substrates did not release critical metals at harmful concentrations, but essential nutrients. It might be an option to leave the substrates where they are and let them slowly cover with silt and mix with the sediment below by bioturbation. Grains that have not weathered at the surface may slowly continue weathering in the sediment, where they actively increase the alkalinity of the salt marsh soil on a long term and in a sustainable manner (e.g., Beerling et al., 2020; Vicca et al., 2022). Further investigations are necessary to evaluate whether enhanced weathering of mafic minerals in the pioneer vegetation zone of salt marshes or the restoration of coastal habitats, in particular mangrove forests and sea grass meadows, is the more cost-effective and environment-friendly solution to sequester atmospheric CO_2 from unavoidable carbon emissions in the future.

Data Available Statement

Data sets for this research are available in the Figshare repository [Datasets] Mendes et al., 2025 https://doi.org/10.6084/m9.figshare.28334438.v2.

References

Abdullayev, E., Baldermann, A., Warr, L. N., Grathoff, G., & Taghiyeva, Y. (2021). New constraints on the palaeo-environmental conditions of the eastern paratethys: Implications from the miocene diatom suite (Azerbaijan). *Sedimentary Geology*, *411*, 105794. https://doi.org/10.1016/j.sedgeo.2020.105794

Allen, J. R. L. (2000). Morphodynamics of holocene salt marshes: A review sketch from the Atlantic and southern north sea coasts of Europe. *Quaternary Science Reviews*, *19*(12), 1155–1231. https://doi.org/10.1016/S0277-3791(99)00034-7

Anschutz, P., & Charbonnier, C. (2020). Sampling pore water at a centimeter resolution in sandy permeable sediments of lakes, streams, and coastal zones. *Limnology and Oceanography: Methods*, *19*(2), 96–114. https://doi.org/10.1002/lom3.10408

Bach, L. T., Gill, S. J., Rickaby, R. E. M., Gore, S., & Renforth, P. (2019). CO_2 removal with enhanced weathering and ocean alkalinity enhancement: Potential risks and Co-benefits for marine pelagic ecosystems. *Frontiers in Climate*, *1*, 7. https://doi.org/10.3389/fclim.2019.00007

Acknowledgments
Researchconducted in the framework of the RECAP project, funded by the Fundação para aCiência e a Tecnologia (FCT), Portugal, under the grant number PTDC/CTA-CLI/1065/2021 (https://doi.org/10.54499/PTDC/CTA-CLI/1065/2021), which also supported J. Lübbers. I. Mendes was supported by the contract CEECINST/00052/2021/CP2792/CT0012 (https://doi.org/10.54499/CEECINST/00052/2021/CP2792/CT0012), A.R. Carrasco by the contract CEECINST/00052/2021/CP2792/CT0007 (https://doi.org/10.54499/CEECINST/00052/2021/CP2792/CT0007), and A. Gomes by the contract CEECINST/00146/2018/CP1493/CT0002 (https://doi.org/10.54499/CEECINST/00146/2018/CP1493/CT0002), all funded by FCT. This study was also supported by FCT national funds under the project UIDB/00350/2020 (https://doi.org/10.54499/UIDB/00350/2020) granted to CIMA BASE and project LA/P/0069/2020 (https://doi.org/10.54499/LA/P/0069/2020) granted to the Associate Laboratory ARNET. The authors acknowledge to the Instituto de Conservação da Natureza e das Florestas, Direção Regional da Conservação da Natureza e Florestas do Algarve (S-026426/2022) and Agência Portuguesa do Ambiente for authorization to carry out the RECAP experiment. The authors also acknowledge to Anke Dettner-Schönfeld for help with logistics and contributions to discussions in an early stage of the project, Andreas Oschlies for valuable suggestions in an early stage of project conceptualization, team members of the RECAP project Óscar Ferreira for valuable contributions to the experiment implantation and Cátia Correia for nutrient analyses and field work participation, Paulo Pedro for valuable discussion and the implementation of the methods applied for chemical analyses in the Laboratory of Chemical Analysis (University of Algarve) and their staff for all the collaboration, and Margarida Ramires for all the collaboration for basalt sieving and cleaning field work material. A special acknowledgment is extended to all the volunteers who participated in the RECAP field work campaigns.

Baldermann, A., Wasser, O., Abdullayev, E., Bernasconi, S., Löhr, S., Wemmer, K., et al. (2021). Palaeo-environmental evolution of central Asia during the cenozoic: New insights from the continental sedimentary archive of the valley of lakes (Mongolia). *Climate of the Past*, *17*(5), 1955–1972. https://doi.org/10.5194/cp-17-1955-2021

Balouin, Y., Howa, H., Pedreros, R., & Michel, D. (2005). Longshore sediment movements from tracers and models, Praia de Faro, South Portugal. *Journal of Coastal Research*, *211*, 146–156. https://doi.org/10.2112/01066.1

Baumann, H., Wallace, R. B., Tagliaferri, T., & Gobler, C. J. (2015). Large natural pH, $CO_2$and O_2 fluctuations in a temperate tidal salt marsh on diel, seasonal, and interannual time scales. *Estuaries and Coasts*, *38*(1), 220–231. https://doi.org/10.1007/s12237-014-9800-y

Beerling, D. J., Kantzas, E. P., Lomas, M. R., Wade, P., Eufrasio, R. M., Renforth, P., et al. (2020). Potential for large-scale CO_2 removal via enhanced rock weathering with croplands. *Nature*, *583*(7815), 242–248. https://doi.org/10.1038/s41586-020-2448-9

Bellamy, R., Chilvers, J., Vaughan, N. E., & Lenton, T. M. (2012). A review of climate geoengineering appraisals, WIREs. *Climate Change*, *3*(6), 597–615. https://doi.org/10.1002/wcc.197

Carrasco, A. R., Kombiadou, K., Amado, M., & Matias, A. (2021). Past and future marsh adaptation: Lessons learned from the Ria Formosa lagoon. *Science of the Total Environment*, *790*, 148082. https://doi.org/10.1016/j.scitotenv.2021.148082

Fakhraee, M., Planavsky, N. J., & Reinhard, C. T. (2023). Ocean alkalinity enhancement through restoration of blue carbon ecosystems. *Nature Sustainability*, *6*(9), 1087–1094. https://doi.org/10.1038/s41893-023-01128-2

Feng, E. Y., Koeve, W., Keller, D. P., & Oschlies, A. (2017). Model-based assessment of the CO_2 sequestration potential of coastal ocean alkalinization. *Earth's Future*, *5*(12), 1252–1266. https://doi.org/10.1002/2017EF000659

Flipkens, G., Blust, R., & Town, R. M. (2021). Deriving nickel (Ni (II)) and chromium (Cr (III)) based environmentally safe olivine guidelines for coastal enhanced silicate weathering. *Environmental Science and Technology*, *55*(18), 12362–12371. https://doi.org/10.1021/acs.est.1c02974

Fuhr, M., Geilert, S., Schmidt, M., Liebetrau, V., Vogt, C., Ledwig, B., & Wallmann, K. (2022). Kinetics of olivine weathering in seawater: An experimental study. *Frontiers in Climate*, *4*, 831587. https://doi.org/10.3389/fclim.2022.831587

Grasshoff, K., Kremling, K., & Ehrhardt, M. (1999). *Methods of seawater analysis*. Wiley. 600.

Guo, J. A., Strzepek, R., Willis, A., Ferderer, A., & Bach, L. T. (2022). Investigating the effect of nickel concentration on phytoplankton growth to assess potential side-effects of ocean alkalinity enhancement. *Biogeosciences*, *19*(15), 3683–3697. https://doi.org/10.5194/bg-19-3683-2022

Hangx, S. J. T., & Spiers, C. J. (2009). Coastal spreading of olivine to control atmospheric CO_2 concentrations: A critical analysis of viability. *International Journal of Greenhouse Gas Control*, *3*(6), 757–767. https://doi.org/10.1016/j.ijggc.2009.07.001

Hartmann, J., West, A. J., Renforth, P., Köhler, P., De La Rocha, C. L., Wolf-Gladrow, D. A., et al. (2013). Enhanced chemical weathering as a geoengineering strategy to reduce atmospheric carbon dioxide, supply nutrients, and mitigate ocean acidification. *Reviews of Geophysics*, *51*(2), 113–149. https://doi.org/10.1002/rog.20004

IPCC. (2018). Global warming of 1.5°C. In *An IPCC Special Report on the impacts of global warming of 1.5°C above pre-industrial levels and related global greenhouse gas emission pathways, in the context of strengthening the global response to the threat of climate change, sustainable development, and efforts to eradicate poverty*. Retrieved from https://www.ipcc.ch/sr15/Köhler

Köhler, P., Abrams, J. F., Völker, C., Hauck, J., & Wolf-Gladrow, D. A. (2013). Geoengineering impact of open ocean dissolution of olivine on atmospheric CO_2, surface ocean pH and marine biology. *Environmental Research Letters*, *8*(1), 014009. https://doi.org/10.1088/1748-9326/8/1/014009

Koop-Jakobsen, K., Mueller, P., Meier, R. J., Liebsch, G., & Jensen, K. (2018). Plant-sediment interactions in salt marshes – Anoptode imaging study of O_2, pH, and CO_2 gradients in the rhizosphere. *Frontiers in Plant Science*, *9*, 541. https://doi.org/10.3389/fpls.2018.00541

Kowalczyk, K. A., Amann, T., Strefler, J., Vorrath, M.-E., Hartmann, J., De Marco, S., et al. (2024). Marine carbon dioxide removal by alkalinization should no longer be overlooked. *Environmental Research Letters*, *19*(7), 074033. https://doi.org/10.1088/1748-9326/ad5192

Le Maitre, R. W. (2005). *Igneous rocks: A classification and glossary of terms: Recommendations of the international union of geological Sciences subcommission on the systematics of igneous rocks* (2nd ed., pp. 1–256). Cambridge University Press. https://doi.org/10.1017/CBO9780511535581

Lewis, E., & Wallace, D. W. R. (1998). *Program developed for CO_2 system calculations, ORNL/CDIAC-105, carbon dioxide information analysis center* (p. 38). Oak Ridge National Laboratory, U.S. Department of Energy.

Meier, F., Rickels, W., Quaas, M. F., & Traeger, C. (2022). *Carbon dioxide removal in a global analytic climate economy (No. 2227)*. Kiel Working Paper.

Meysman, F. J. R., & Montserrat, F. (2017). Negative CO_2 emissions via enhanced silicate weathering in coastal environments. *Biology Letters*, *13*(4), 20160905. https://doi.org/10.1098/rsbl.2016.0905

Montserrat, F., Renforth, P., Hartmann, J., Leermakers, M., Knops, P., & Meysman, F. J. R. (2017). Olivine dissolution in seawater: Implications CO_2 sequestration through enhanced weathering in coastal environments. *Environmental Science and Technology*, *51*(7), 3960–3972. https://doi.org/10.1021/acs.est.6b05942

Morrow, D. R., Thompson, M. S., Anderson, A., Batres, M., Buck, H. J., Dooley, K., et al. (2020). Principles for thinking about carbon dioxide removal in just climate policy. *One Earth*, *3*(2), 150–153. https://doi.org/10.1016/j.oneear.2020.07.015

National Research Council. (2015). *Climate intervention: Carbon dioxide removal and reliable sequestration*. The National Academies Press. https://doi.org/10.17226/18805

Pavlova, G. Y., Tishchenko, P. Y., Volkova, T. I., Dickson, A., & Wallmann, K. (2008). The intercalibration of measurement techniques for total alkalinity in seawater. *Oceanology*, *48*, 460–465.

Poate, T. G., Masselink, G., Russell, P. E., & Austin, M. J. (2014). Morphodynamic variability of high-energy macrotidal beaches, Cornwall, UK. *Marine Geology*, *350*, 97–111. https://doi.org/10.1016/j.margeo.2014.02.004

Reithmaier, G. M. S., Cabral, A., Akhand, A., Bogard, M. J., Borges, A. V., Bouillon, S., et al. (2023). Carbonate chemistry and carbon sequestration driven by inorganic carbon outwelling from mangroves and saltmarshes. *Nature Communications*, *14*(1), 8196. https://doi.org/10.1038/s41467-023-44037-w

Renforth, P., & Henderson, G. (2017). Assessing ocean alkalinity for carbon sequestration. *Reviews of Geophysics*, *55*(3), 636–674. https://doi.org/10.1002/2016RG000533

Rogelj, J., Elzen, M., Höhne, N., Fransen, T., Fekete, H., Winkler, H., et al. (2016). Paris Agreement climate proposals need a boost to keep warming well below 2°C. *Nature*, *534*(7609), 631–639. https://doi.org/10.1038/nature18307

Saderne, V., Fietzek, P., & Herman, P. M. J. (2013). Extreme variations of pCO_2 and pH in a macrophyte meadow of the baltic sea in summer: Evidence of the effect of photosynthesis and local upwelling. *PLoS One*, *8*(4), e62689. https://doi.org/10.1371/journal.pone.0062689

Schönfeld, J., & Mendes, I. (2022). Benthic foraminifera and pore water carbonate chemistry on a tidal flat and salt marsh at Ria Formosa, Algarve, Portugal. *Estuarine, Coastal and Shelf Science*, *276*, 108003. https://doi.org/10.1016/j.ecss.2022.108003

Schuiling, R. D., & de Boer, P. L. (2011). Rolling stones; fast weathering of olivine in shallow seas for cost-effective CO_2 capture and mitigation of global warming and ocean acidification. *Earth System Dynamics*, *2*, 551–568. https://doi.org/10.5194/esdd-2-551-2011

Schulz, H. D. (2006). Quantification of early diagenesis: Dissolved constituents in pore water and signals in the solid phase. In H. D. Schulz & M. Zabel (Eds.), *Marine geochemistry* (pp. 73–124). Springer Berlin Heidelberg.

Schunter, C., Jarrold, M. D., Munday, P. L., & Ravasi, T. (2020). Diel pCO_2 fluctuations alter the molecular response of coral reef fishes to ocean acidification conditions. *Molecular Ecology*, *30*(20), 5105–5118. https://doi.org/10.1111/mec.16124

Seeberg-Elverfeldt, J., Schlüter, M., Feseker, T., & Kölling, M. (2005). A Rhizon in situ sampler (RISS) for pore water sampling from aquatic sediments. *Limnology and Oceanography: Methods*, *3*, 361–371. https://doi.org/10.4319/lom.2005.3.361

Simon, M., Grossart, H. P., Schweitzer, B., & Ploug, H. (2002). Microbial ecology of organic aggregates in aquatic ecosystems. *Aquatic Microbial Ecology*, *28*, 175–211. https://doi.org/10.3354/ame028175

Strefler, J., Amann, T., Bauer, N., Kriegler, E., & Hartmann, J. (2018). Potential and costs of carbon dioxide removal by enhanced weathering of rocks. *Environmental Research Letters*, *13*(3), 034010. https://doi.org/10.1088/1748-9326/aaa9c4

Ten Berge, H. F., Van der Meer, H. G., Steenhuizen, J. W., Goedhart, P. W., Knops, P., & Verhagen, J. (2012). Olivine weathering in soil, and its effects on growth and nutrient uptake in ryegrass (lolium perenne L.): A pot experiment. *PLoS One*, *7*(8), e42098. https://doi.org/10.1371/journal.pone.0042098

United Nations Framework Convention on Climate Change. (2015). Adoption of the Paris agreement. *Report No. FCCC/CP/2015/L.9/Rev.1*. Retrieved from http://unfccc.int/resource/docs/2015/cop21/eng/l09r01.pdf

van der Jagt, H., Friese, C., Stuut, J.-B., Fischer, G., & Iversen, M. H. (2018). The ballasting effect of Saharan dust deposition on aggregate dynamics and carbon export: Aggregation, settling, and scavenging potential of marine snow. *Limnology & Oceanography*, *63*(3), 1386–1394. https://doi.org/10.1002/lno.10779

Vicca, S., Goll, D. S., Hagens, M., Hartmann, J., Janssens, I. A., Neubeck, A., et al. (2022). Is the climate change mitigation effect of enhanced silicate weathering governed by biological processes? *Global Change Biology*, *28*(3), 711–726. https://doi.org/10.1111/gcb.15993

Vink, J. P. M., & Knops, P. (2023). Size-fractionated weathering of olivine, its CO_2-sequestration rate, and ecotoxicological risk assessment of nickel release. *Minerals*, *13*(2), 235. https://doi.org/10.3390/min13020235

Walker, G. P. L. (1992). Puu Mahana near South Point in Hawaii is a primary Surtseyan ash ring, not a sandhills-type littoral cone. *Pacific Science*, *46*(1), 1–10. http://hdl.handle.net/10125/1669

Wallmann, K. (2023). Method/description alkalinity. last access https://www.geomar.de/en/research/fb2/fb2-mg/benthic-biogeochemistry/mg-analytik/alkalinity#c13229 17 06 2023.

Wallmann, K., Aloisi, G., Haeckel, M., Obzhirov, A., Pavlova, G., & Tishchenko, P. (2006). Kinetics of organic matter degradation, microbial methane generation, and gas hydrate formation in anoxic marine sediments. *Geochimica et Cosmochimica Acta*, *70*(15), 3905–3927. https://doi.org/10.1016/j.gca.2006.06.003

Wright, L., & Short, A. (1984). Morphodynamic variability of surf zone and beaches: A synthesis. *Marine Geology*, *56*(1–4), 93–118. https://doi.org/10.1016/0025-3227(84)90008-2